Identification of Triassic Braided River Sedimentary Facies in Tarim Basin: A Case Study

*Lingting Zhang, **Guiyu Dong, ***Xiangxin Lv, ****Chunpeng Leng

*School of Mining Engineering, North China University of Science and Technology, Tangshan 063000, China (zhang2008lt@163.com)
**School of Mining Engineering, North China University of Science and Technology, Tangshan 063000, China (dguiyuchengdu@sina.com)
***School of Mining Engineering, North China University of Science and Technology, Tangshan 063000, China (liuxiangxin9@163.com)
****School of Mining Engineering, North China University of Science and Technology, Tangshan 063000, China (377905101@qq.com)

Abstract

The Triassic sedimentary facies in the Tarim Basin encompasses such three facies as braided river, braided river delta and coastal shallow lake. Targeted at the lowstand systems tract (LST) sandbodies in SQ3 sequence, lower oil formation of Akekule region, the author prepared the 3-end-member diagram of rock-mineral components, the ertzsprung–RussellH diagram and the cumulative probability curve diagram, and applied these diagrams in the compressive analysis on the features of the braided river facies in the region. The analysis shows that the braided river facies bear the following distinctive features: the lack of diversity in rock type (the region is dominated by fine- to medium- grained feldspar lithic sandstone), low compositional maturity, high content of matrix and cement, low structural maturity (the grains are mainly sub-prismatic and sub-rounded), rich sedimentary structure (there is an unobvious "binary structure"), low gamma-ray and resistivity values. The braided river sedimentation pattern was then summed up in a sedimentary facies diagram, which reveals that the braided river sandbodies are distributed annularly, and the sandbody thickness gets thinner in the north-south direction.

Key words

Tarim basin, Triassic system, Akekule region, Low Systems Tract (LST), Braided river, Sedimentary facies.

1. Introduction

Braided rivers are often wide and shallow, featuring multiple channels, a steep channel gradient, and rapid lateral migration [1,2]. Being an important part of continental deposition, the braided river sedimentary facies is so complex that it varies with region and time [3-6]. The sedimentation pattern bears some differences from the classical model proposed by Walker, R.G. and Cant, D.J. [7]. The existing studies on the Triassic sedimentary facies in the Tarim Basin are mainly concentrated in the braided river facies and sublacustrine fan facies in the upper to medium oil formations of Akekule Region [8-10]. The braided rivers develop mainly in resource-rich provenances, which are linearly distributed in the piedmont zone on the margin of basins, and in close proximity to braided river deltas. Due to the seasonal runoff variation and frequent clustering and dispersion of channels, the channel bars are much more developed than point bars I the braided rivers. The braided river sedimentary facies has an incomplete binary structure, as the soil is sandwiched between sand. Whereas the sedimentary characteristics are affected by various factors like season, region, and provenance, it is very meaningful to identify braided rivers correctly, and sum up its development features. The results may help to predict whether a region is an oil and gas-bearing zone.
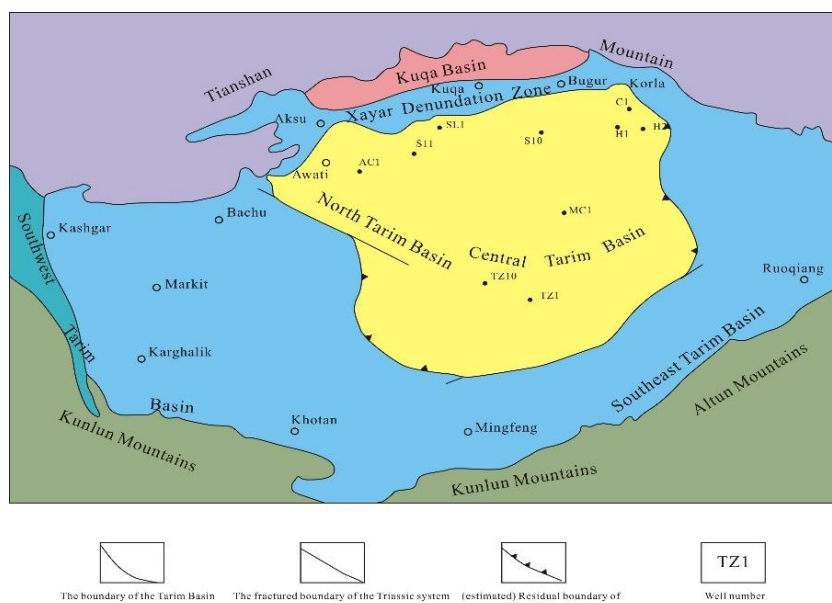
2. Geological Profile

Fig.1. Distribution of the Remaining Triassic Strata in the Tarim Basin

As the largest petroliferous basin in Chinese inland, the Tarim Basin is an east-west trending basin, covering an area of $56 \times 10^4 km^2$. With Tianshan fold system in the north and the Kunlun fold system in the south, the basin consists of "two uplifts and two depressions", a total of four primary tectonic units. It is worth mentioning that, the Triassic system, belonging to the fourth tectonic layer created by the convergence of the Paleo-Tethys Ocean, does not exist in most places of the basin. The only remnant of the system lies in the south of the north Tarim uplift, the Awati depression, the midsection of the central Tarim uplift, and the Kuqa depression. Specifically, the system thickness approximates 1,000m in the Awati depression, and peaks at 1,500m in the Kuqa depression. This study focuses on the Akekule uplift, which is situated on the southwest wing of the midsection of north Tarim uplift (the Xayar uplift) [12, 13]. As shown in Figure (1), the Triassic strata has been discovered from S14 well in the north to TZ1 well in the south, and from the AC1 well in the west to the M2 well in the east.

3. Regional Sedimentation System

The Triassic system in the study area is composed of three layers, namely, the Upper Triassic Halahatang Formation, the Middle Triassic Akekule Formation and the Lower Triassic Ketur Formation. The system can also be divided into the upper, medium and lower oil formations [12,14]. The lower oil formation is made up of the upper sandstone section of Akekule Formation. Using Vial's classical sequence stratigraphic pattern and the sinusoidal eustatic curve, Liu Qingsheng et al. classified the Triassic system into six tertiary sequences from bottom to top, and denoted them as SQ1, SQ2, SQ3, SQ4, SQ5, and SQ6 [14]. In the SQ3 sequence, the low systems tract (LST) is extremely well developed, the transgressive systems tract (TST) is well developed while the high systems tract (HST) is not developed.

Through the analysis of field outcrop, core wafer and logging response, it is concluded that the braided river is the dominant sedimentary system of the LST sandbodies in SQ3 sequence, lower oil formation of the Triassic system. The braided river channels contain coarse-grained sediments, including grain-bearing coarse, medium and fine sandstones. Large oblique bedding, tabular cross-bedding and parallel bedding were formed in the channels. It is rare to find any ancient fossil in the beddings. The sedimentary subfacies between the channels is featured by a thin layer of mudstone left by the fluvial incision, which contains slices of plant stems. Overall, the braided river facies has obvious sedimentary rhythm, and a coarser grainsize in the upper sequences. From the 2D angle, the LST sandbodies are thicker in the north than the south, with an average thickness of over 30m. The LST mostly carries the channel-filling sediments of the braided rivers that eroded the gullies in late Triassic Period.

4. Identification of Braided River Sedimentary Facies

4.1 Rock Type

The author collected over 40 samples from nearly 10 wells, performed thin-section identification of these samples, and analysed the grainsize of 3 wells (Figure 2). The results show that: the sandbodies deposited in braided rivers have relatively rough grainsize; the rocks include feldspar lithic sandstone, lithic quartz sandstone, lithic feldspar sandstone, lithic sandstone and a few feldspars; the lithic fragment content is greater than feldspar content; the feldspar lithic sandstone is the dominant type of rock. According to the thin-section identification: the content of quartz (Q) is 48.57%~55.26%, the content of feldspar (F) is 18.24%~22.4%, the content of rock fragments (R) is 26.03~29.3% and the matrix content is 8.84~0.85%. Thus, fine-to medium-grained sandstones (common grainsize: 0.35~0.7mm; max grainsize: 1~7.6mm) make up most of the sedimentary rocks, plus a few conglomerates and mudstones. To sum up, the rocks deposited in the river channels of the study area are dominated by medium-grained (including fine grained) feldspar lithic sandstone (Attached Figure a).
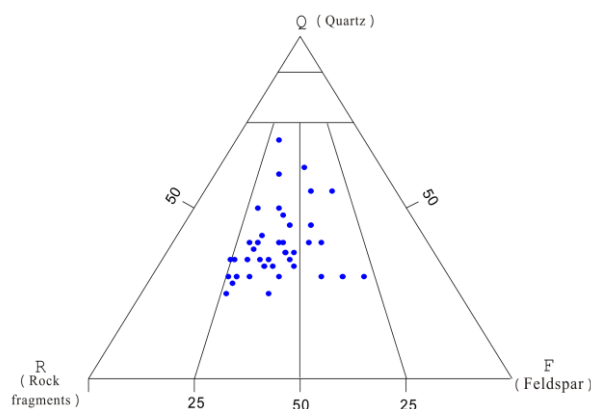

Fig.2. The 3-end-member Diagram of Rock-mineral Components in Lower Oil Formation of Triassic System

4.2 Sandstone Composition Maturity

The rock samples contain about 48% of quartz with developed intergranular pores. According to the statistics on heavy minerals, the content of heavy minerals is averaged at 0.79%. The samples mainly consist of stable minerals like zircon (16.3%), rutile (0.86%), tourmaline (3.48%) and garnet (61.3%) and unstable minerals like titanite (83.6%), zoisite (3.31%) and a small amount of glauconite, plus trace amounts of iron-rich pyrite in local areas. On the whole, the quartz and feldspar contents are much lower than the rock fragment content; the average mineral maturity is 0.22; the heavy mineral assemblage is featured by the coexistence of stable and unstable minerals,

acidic igneous rock, and metamorphic rock minerals. Therefore, the sandstone in the study area is low in maturity.

4.3 Matrix Content and Cement Content

Most of the matrix is argillaceous and most of the cement is calcareous. The average content of matrix and cement amounts to 18.6%. The grain-supported structure is much more prevalent than the porous cementation. In the interstitial material of the grain-supported structure, the matrix is mainly argillaceous (Attached Figure b), taking up 0.5%~50% of the interstitial material. With an average content of 9%, the cement is mainly calcareous, including a small amount of kaolinite, chlorite, and calcite. The porous cementation is the dominant way of cementation, supplemented by individual porous-matrix cementation.

4.4 Structural Maturity

According to the thin-section identification, the clastic grains are coarse, with an average grainsize of 0.09~7.6, fine-to medium-grained, poorly-well sorted, moderate in roundness and mainly sub-prismatic and sub-rounded. This means the rocks have an extremely low structural maturity (Attached Figure d). Figure 3 presents the cumulative probability curve of the LST sandbodies in sequence SQ3, Triassic system in well S10. It can be seen that the middle to high sloped curve is distributed in a two-stage form; the jumping population takes up more than 85% of all populations, followed by the suspension population; there is no rolling population. The intercept point between the jumping and suspension populations appears in the interval of 3.6~3.9φ. The above phenomena demonstrate a low structural maturity and the effect of traction current deposition.

The Hertzsprung–Russell diagram below also evidences that the LST sandbodies in SQ3 sequence, lower oil formation, formed the braided river facies under the effect of traction current deposition. In the Hertzsprung–Russell diagram, the PQ and QR sections signify well development. The QR section is parallel to the C=M line, indicating that traction flow deposition has a similar effect with sand bar deposition in river channels (Figure 4).

4.5 Sedimentary Structure

Through the observation of the core, it is learned that the Triassic sedimentary structure is extremely well developed. The parallel bedding and carbonaceous lamina, commonly seen in fine sandstones, concentrate in sedimentary strata with fine grainsize and shallow waterbodies, such as the fine sandstone and muddy siltstone at the top of channel bars; the oblique bedding, cross-

bedding and ripple cross-lamina are developed in siltstone, sandstone, and gravel-bearing sandstone. The "binary structure" is unobvious, as fine sandstone and coarse sandstone are respectively above and below the erosion surface. The mudstone contains no bedding and sporadic water escape structures, while the sand bodies exhibit lots of developed parallel and oblique beddings. Such a sedimentary structure reveals relatively strong hydrodynamic force at the time of deposition (Attached Figures c~g)
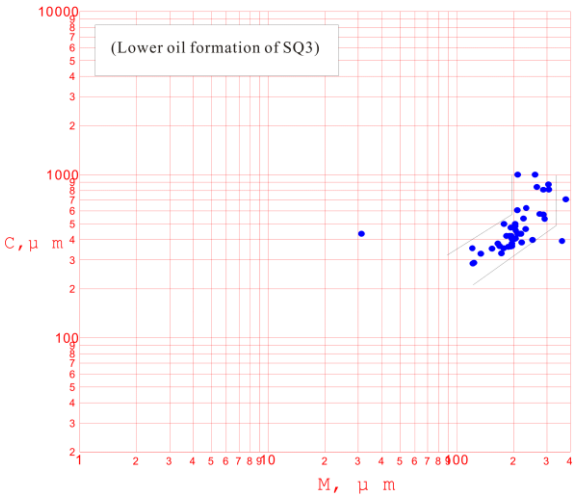

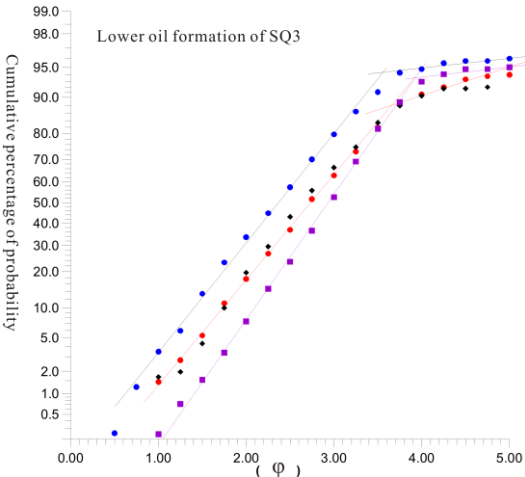Fig.3. The Cumulative Probability Curve Diagram of LST Sandbodies in SQ3 Sequence of Triassic System in S10 Well

Fig.4. The Hertzsprung-Russell Diagram of LST Sandbodies in SQ3 Sequence, Lower Oil Formation of Triassic System

4.6 Logging Curves

In AT1 well, S10 well, Shun-8 well and the other five wells, the logging curves of LST sandbodies in SQ3 sequence exhibit abnormal SP curves and low gamma-ray and resistivity values (Figure 5); the logging wells gradually change from micro-jugged box shape to the coexistence of bell shape, figure shape and micro-jugged box shape. The SP curve of channel sedimentation is either the combination of micro-jugged box shape-finger shape- micro-jugged box shape, or the

combination of box shape and bell shape. The curve shapes imply a normal graded bed sequence with gradual weakening of hydrodynamic force after the rapid accumulation of sediment or stabilization of hydrodynamic conditions, and the emergence of thin-layers of mudstone in local areas under hydrostatic deposition in the brief low-energy environment. The GR curve can be subdivided into several small bell-shaped segments, indicating that the cyclothem interfaces become more continuous as the depth decreases under the combined effect of several channel depositions. The logging curve characteristics of braided channels manifest the abundant resources of the provenance, sharp fluctuation of hydrodynamic energy in a short period, and relatively fast deposition rate.
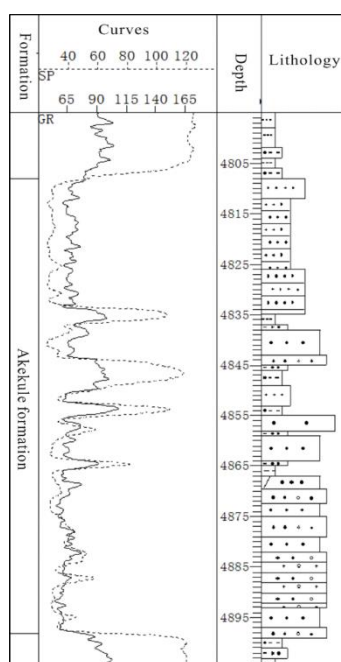

Fig.5. Composite Histogram on Braded River Sedimentation of LST Sandbodies in SQ3 Sequence, Lower Oil Formation of Triassic System in S99 Well

5. Sendimentary Pattern

The Triassic system in the study area is a braided river-braided river delta-lake sedimentary system. Through the sequence stratigraphic analysis [8, 9-11] (Figure 6), it is concluded that: with the decline of the lake level (LST), the area is basically the raided river deposition system; thanks to the rapid migration and extension of the braided system, the LST sandbodies are easy to track and compare across the study area. With the rapid rise of the lake (TST), the study area is flooded by the lake. In this case, the study area bears the features of lake sedimentary system.
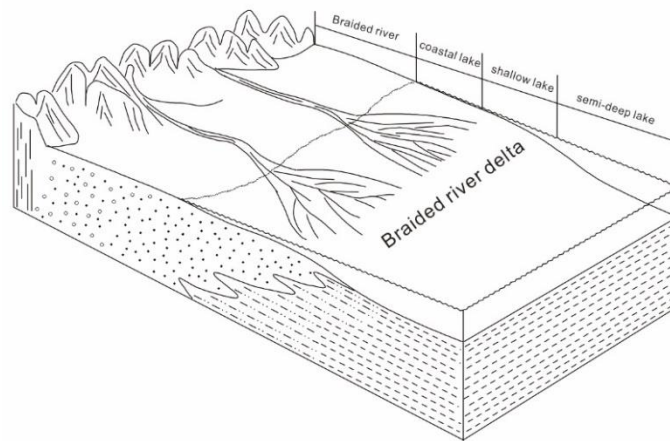
Fig.6. Sedimentary Pattern of the Triassic System in Akekule Uplift

6. Planar Distribution of Sedimentary Facies

In the SQ3 sequence, the LST is developed, the TST is not developed and the HST is absent. The LST is formed with channel sandbodies at the lower part of the lower oil formation of Triassic system. The Triassic system of the study area is dominated by braided river sedimentary facies, plus some braided river delta facies in local areas (Figure 7). The extremely well developed braided river facies advances from the northwest into the water bodies, creating an annular distribution of braided river channel sandbodies.
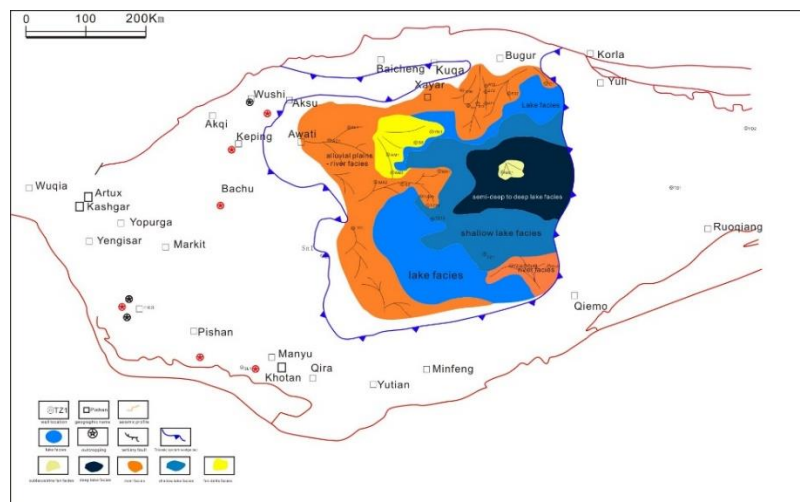

Fig.7. Planar Diagram of LST Sedimentary Facies in SQ3 Sequence, Lower Oil Formation of Triassic System in the Tarim Basin

Conclusion

1. Through the thin-section identification and grainsize analysis, it is concluded that: the sandbodies deposited in braided rivers have relatively rough grainsize; the feldspar lithic sandstone is the dominant type of rock. the rocks deposited in the river channels of the study area are

dominated by medium-grained (including fine grained) feldspar lithic sandstone. The sandstone in the study area is low in maturity, for the heavy mineral assemblage is featured by the coexistence of stable and unstable minerals, acidic igneous rock, and metamorphic rock minerals.

2. Most of the matrix is argillaceous and most of the cement is calcareous. The porous cementation is the dominant way of cementation, supplemented by individual porous-matrix cementation. The clastic grains are coarse, fine-to medium-grained, poorly-well sorted, moderate in roundness and mainly sub-prismatic and sub-rounded. The above features demonstrate a low structural maturity and the effect of traction current deposition.

3. The "binary structure" is unobvious, as fine sandstone and coarse sandstone are respectively above and below the erosion surface. The mudstone contains no bedding and sporadic water escape structures, while the sand bodies exhibit lots of developed parallel and oblique beddings. Such a sedimentary structure reveals relatively strong hydrodynamic force at the time of deposition.

4. The abnormal logging curve characteristics of braided channels manifest the abundant resources of the provenance, sharp fluctuation of hydrodynamic energy in a short period, and relatively fast deposition rate.

5. The Triassic system in the study area is a braided river-braided river delta-lake sedimentary system. The dominance of braided river sedimentary facies is supplemented by some braided river delta facies in local areas. The extremely well developed braided river facies advances from the northwest into the water bodies, creating an annular distribution of braided river channel sandbodies. The sandbody thickness gets thinner in the north-south direction.

Attached Figure

a

b
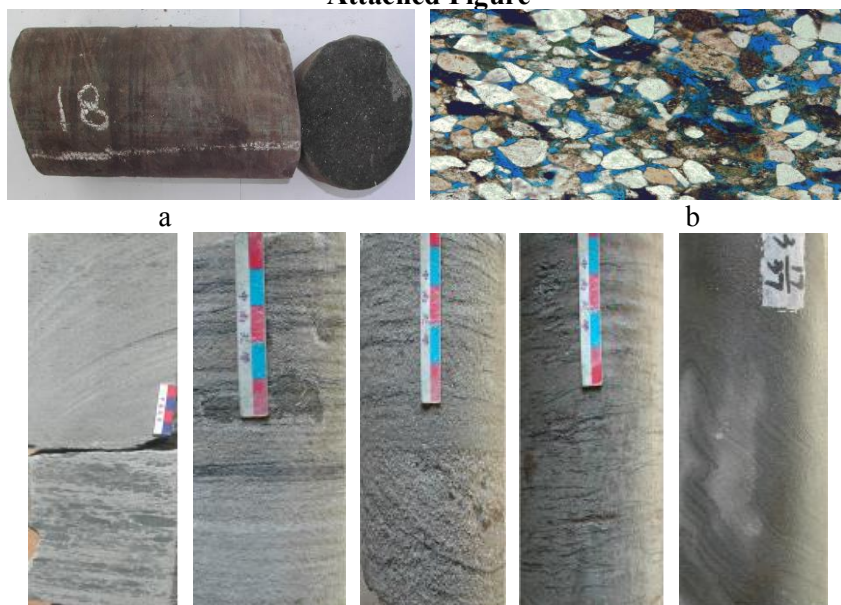
c   d   e   f   g

Note

a. The microfacies of braided river deposition of a channel bar. The rock is a light grey medium-grained calcareous feldspathic litharenite. Calcareous fragments are observable on the surface. The core is loose and the surface was dyed brown by mud.

b. The microscopic lithology characteristics of S113 well (4,462.52m): the rocks are fine- to medium-grained feldspar lithic sandstone; the cement includes kaolinite (0.5%) and argillaceous matrix (1%). The estimated surface porosity is 20%. The pores are evenly distributed, and mainly exist as intergranular pores. There are also small amounts of intra-granular pores and intergranular micropores of kaolinite, a few micropores on the matrix and rock fragments, as well as sporadic mould pores and particle fissures.

c. The boulder clay and medium-grained sandstone in braided river channel of lower oil formation in AT1 well (4,315.01m).

d. The parallel bedding and carbonaceous lamina in fine-grained sandstone of S100 well.

e. The erosion surface, oblique bedding and cross-bedding of S100 well. The fine sandstone and coarse sandstone are respectively above and below the erosion surface.

f. The ripple cross-lamina in the argillaceous siltstone of S100 well.

g. The water escape structures in the argillaceous siltstone of S100 well.

References

1. H.E. Wheeler, Base level, lithosphere surface and time-stratigraphy, 1964, Bull Geol Soc, vol. 75, pp. 599-610.

2. P.R. Vail, R.M. Mitchum, R.G. Todd, Seismic stratigraphy and global changes of sea level, 1977, In: Payton C E, eds, Seismic stratigraphy- applications to hydrocarbon exploration, AAPG, Memoir, no. 26, pp. 49- 212.

3. S.F. Mtichell, C.R. Paul, A.S. Gale, Carbon isotopes and sequence stratigraphy, 1996, High resolution sequence stratigraphy: Innovations and applications, Geo logical Society Special Publication, no. 104, pp. 11-24.

4. J.M. Armentrout, High resolution sequence bio stratigraphy: Examples from the Gulf of Mexico Plio－Pleistocene, High resolution sequence stratigraphy: Innovations and applications, Geological Society Special Publication, no. 104, pp. 65-86.

5. W.E. Galloway, Genetic stratigraphic sequence in basin analysis l: Architecture and genesis of flooding/surface bounded depositional units, 1989, AAPG Bull, vol. 73, pp. 125-142.

6. T. Olsen, R. Steel, K. Hogseth, Sequential architecture in a fluvial succession: sequence stratigraphy in the Upper Cretaceous Mesaverde Group, Price Canyon, Utah, 1995, Journal of Sedimentary Research, vol. 65, no. 2b, pp. 265-280.

7. D.J. Cant, R.G. Walker, Development of a braided fluvial facies model for the Devonian Battery Point sandstone, 1976, Quebec: Canadian Journal of Earth Science, vol. 13, pp. 102-119.

8. C.S. Lv, J.H. Guo, R. Zhu, Study on sedimentary facies of the middle oil group of the Triassic in Akekule area of Tarim Basin, 2007, Journal of Xi'an Shiyou University (Natural Science Edition), vol. 22, no. 6, pp. 36-40.

9. C.S. Lv, J.H. Guo, Probe Into Sublacustrine Fan of Triassic in Akekule area, Tarim Basin, 2008, Xi'an Shiyou University (Natural Science Edition), no. 3, pp. 17-19.

10. H. Zhu, The study on the sedimentary and sequence stratigraphy characteristics and source-reservoir-caprock assemblages of the triassic at the tabei-tazhong area, Tarim Basin, 2011, Chengdu University of Technology.

11. J.Z. Zhao, Petroleum geologic features of Tarim Basin, 1997, Xi'an Shiyou University, vol. 12, no. 2, pp. 8-15.

12. Y.C. Zhou, G.L. Yang, The character and prospect of the petroleum etroleum geology of the area of Akekule in Tarim Basin, 2001, Acta Petrolei Sinica, no. 3, pp. 1-5.

13. Y.P. Feng, The control action of tectonic evolution over oil and gas in Akekule lobe of Tarim Basin, 2012, Chengdu University of Technology.

14. C.S. Lv, Study of sequence stratigraphy and sedimentary facies of Triassic System of Akekule area in Tarim basin, 2006, Central South University.